tvst

https://doi.org/10.1167/tvst.8.5.21

Article

Assessing the Interocular Symmetry of Foveal Outer Nuclear Layer Thickness in Achromatopsia

Rebecca R. Mastey[1], Mina Gaffney[1], Katie M. Litts[1], Christopher S. Langlo[2], Emily J. Patterson[1], Margaret R. Strampe[1,3], Angelos Kalitzeos[4,5], Michel Michaelides[4,5], and Joseph Carroll[1,2]

[1] Ophthalmology & Visual Sciences, Medical College of Wisconsin, Milwaukee, WI, USA
[2] Cell Biology, Neurobiology, & Anatomy, Medical College of Wisconsin, Milwaukee, WI, USA
[3] University of Minnesota Medical School, Minneapolis, MN, USA
[4] Institute of Ophthalmology, University College London, London, EC1V 9EL, UK
[5] Moorfields Eye Hospital, London, EC1V 2PD, UK

Correspondence: Joseph Carroll, Department of Ophthalmology & Visual Sciences, Medical College of Wisconsin, 925 N 87th St, Milwaukee, WI 53226-0509, USA. e-mail: jcarroll@mcw.edu

Received: 14 February 2019
Accepted: 12 August 2019
Published: 2 October 2019

Keywords: achromatopsia; outer nuclear layer; optical coherence tomography

Citation: Mastey RR, Gaffney M, Litts KM, Langlo CS, Patterson EJ, Strampe MR, Kalitzeos A, Michaelides M, Carroll J. Assessing the interocular symmetry of foveal outer nuclear layer thickness in achromatopsia. Trans Vis Sci Tech. 2019;8(5):21, https://doi.org/10.1167/tvst.8.5.21

Purpose: We examine the interocular symmetry of foveal outer nuclear layer (ONL) thickness measurements in subjects with achromatopsia (ACHM).

Methods: Images from 76 subjects with *CNGA3*- or *CNGB3*-associated ACHM and 42 control subjects were included in the study. Line or volume scans through the fovea of each eye were acquired using optical coherence tomography (OCT). Image quality was assessed for each image included in the analysis using a previously-described maximum tissue contrast index (mTCI) metric. Three foveal ONL thickness measurements were made by a single observer and interocular symmetry was assessed using the average of the three measurements for each eye.

Results: Mean (± standard deviation) foveal ONL thickness for subjects with ACHM was 79.7 ± 18.3 μm (right eye) and 79.2 ± 18.7 μm (left eye) compared to 112.9 ± 15.2 (right eye) and 112.1 ± 13.9 μm (left eye) for controls. Foveal ONL thickness did not differ between eyes for ACHM ($P = 0.636$) or control subjects ($P = 0.434$). No significant relationship between mTCI and observer repeatability was observed for either control ($P = 0.140$) or ACHM ($P = 0.351$) images.

Conclusions: While foveal ONL thickness is reduced in ACHM compared to controls, the high interocular symmetry indicates that contralateral ONL measurements could be used as a negative control in early-phase monocular treatment trials.

Translational Relevance: Foveal ONL thickness can be measured using OCT images over a wide range of image quality. The interocular symmetry of foveal ONL thickness in ACHM and control populations supports the use of the non-study eye as a control for clinical trial purposes.

Introduction

Achromatopsia (ACHM) is an autosomal recessive inherited cone dysfunction syndrome, affecting approximately 1 in 30,000 people worldwide.[1] It is characterized by increased light sensitivity, reduced visual acuity, nystagmus, and reduced or absent color vision. To date, mutations in six genes have been associated with ACHM: *CNGA3*, *CNGB3*, *GNAT2*, *PDE6C*, *PDE6H*, and *ATF6*[2–5]— with *CNGA3* and *CNGB3* mutations accounting for nearly 70% of all ACHM cases.[6] While ACHM generally is thought to be stable, there are conflicting reports regarding the progressive nature of ACHM.[7–11] The recent success of gene therapy in the mouse, canine, and sheep models of ACHM[12–14] has made ACHM a well-suited disease for exploring gene therapy options in humans. Indeed, a number of gene therapy trials are underway seeking to restore cone function in patients with ACHM.[15,16] However a prerequisite for therapeutic success is that the individual retina being treated contains residual cone photoreceptors.

Table 1. Subject Characteristics

Parameter	Control	ACHM	*P* Value*
Sex	19M, 23F	38M, 38F	0.702
Gene affected	NA	14 *CNGA3*, 62 *CNGB3*	NA
Age, yrs (mean ± SD)	26.7 ± 9.7	24.1 ± 13.5	0.064
Axial length, mm (mean ± SD)			
Right eye	24.1 ± 1.25	23.9 ± 1.87	0.166
Left eye	24.1 ± 1.27	23.8 ± 1.89	0.088

M, male; F, female; NA, not applicable.
* See text for specific statistical tests used.

A variety of imaging approaches have been used to examine remnant cone structure in patients with ACHM. While confocal adaptive optics scanning light ophthalmoscopy (AOSLO) imaging reveals an absence of normal waveguiding cones in patients with *CNGA3*- and *CNGB3*-associated ACHM,[17–19] nonconfocal split-detector AOSLO imaging has been used to show extensive, yet variable, residual cone inner segment structure in these patients.[19–21] However, even nonconfocal split-detector AOSLO-based estimates of remnant cone structure may underestimate the therapeutic potential of a given retina. This is evidenced in a variety of diseases where outer segment shortening and inner segment swelling precede the final loss of the cone nucleus.[22–25] Therefore, assessing the thickness of the foveal outer nuclear layer (ONL), comprised primarily of cone nuclei, may provide important auxiliary information regarding remnant cone structure in patients with ACHM.

Optical coherence tomography (OCT) has been used for analysis of many features within the macular region of patients with ACHM, including ellipsoid zone integrity, foveal hypoplasia, and foveal ONL thickness.[26,27] Patients with *CNGA3*- and *CNGB3*-associated ACHM show significant thinning of the ONL compared to controls.[19,26–28] A recent study found no interocular difference in foveal ONL thickness in seven subjects with *CNGA3*-associated ACHM,[21] though interocular symmetry has not been assessed across a larger group of subjects. As the progressive nature of cone degeneration in ACHM remains unsettled (and may vary on a patient-by-patient basis), determining the degree of ONL symmetry is important for any trials where one eye is treated and the other is used for comparison. Here, we used OCT to examine the interocular symmetry of the ONL at the fovea in subjects with *CNGA3*- and *CNGB3*-associated ACHM using custom software (OCT Reflectivity Analytics; ORA).[29]

Materials and Methods

Subjects

This research followed the tenets of the Declaration of Helsinki and was approved by the institutional review boards at Moorfields Eye Hospital (MEH) and Medical College of Wisconsin (MCW; PRO0017439 and PRO00030741). Images from 76 subjects (17 from MEH and 59 from MCW) genetically confirmed to have *CNGA3*- or *CNGB3*-associated ACHM were used for this study and 42 subjects (all from MCW) with normal vision were used as controls. The demographics of the subject populations are shown in Table 1. If a patient had multiple visits during which both eyes were imaged, the date used for analysis chosen as the one with the best image quality (assessed subjectively by a single observer, RRM), with priority given to the most recent date. Subjects with ACHM who had macular atrophy (i.e., grade 5 ellipsoid zone disruption[27]) were excluded from the study as it is not possible to measure the ONL in these retinas. The controls were not recruited in any specific or systematic manner, rather selected from prior studies in which the subject agreed to have their OCT images used for future unspecified research (i.e., banked) and for whom good quality (again assessed subjectively by a single observer, RRM) line scans were available. Axial length was measured for each subject using an IOL Master (Carl Zeiss Meditec, Dublin, CA).

OCT Imaging and Processing

Before imaging, all subjects with ACHM were dilated using either a single drop of cyclomydril (cyclopentolate hydrochloride [0.2%] and phenyleph-

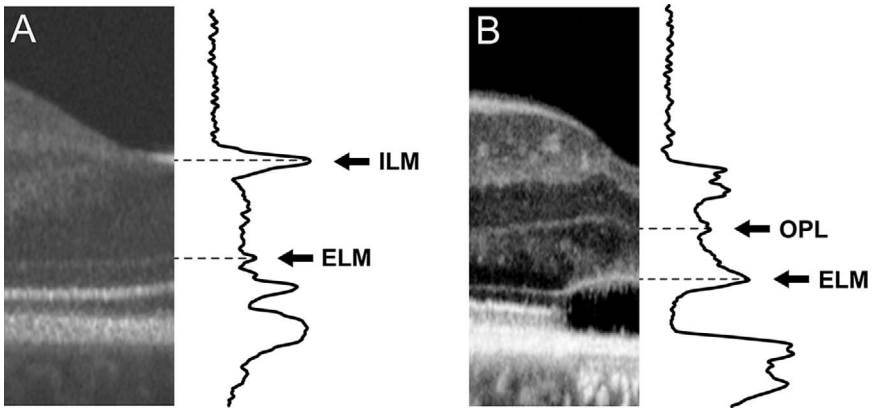

Figure 1. Demonstration of measuring ONL thickness in cases without hypoplasia and with hypoplasia. When hypoplasia is not present (A), the ONL is defined as the distance between the ELM and the ILM. When hypoplasia is present (B), the ONL then is defined as the distance between the ELM and the next boundary, which is the OPL.[27,43] Images are displayed and were measured using a logarithmic scale.

rine hydrochloride [1%]) or a combination of tropicamide (1%) and phenylephrine hydrochloride (2.5%) for cycloplegia and pupillary dilation. Control subjects were imaged without dilation, as a previous study evaluated layer thickness measurements before and after dilation and found no change.[30] The Bioptigen spectral domain OCT (Leica Microsystems, Wetzlar, Germany) was used to acquire transfoveal line and/or volume scans in both eyes of each subject. For the 42 control subjects, horizontal line scans (1000 A-scans per B-scan, 80–100 repeated B-scans) were acquired with a nominal scan length of 7 mm. Multiple B-scans (n = 2–20) were registered and averaged in ImageJ[31] to create a single .tif image, or processed line scan, with improved contrast for analysis, as previously reported.[32,33] For the 76 subjects with ACHM, the image acquisition was more variable, owing to the multiple sites and longer timeframe over which the images were collected. Horizontal line scans (1000 A-scans per B-scan, 80–100 repeated B-scans) were acquired with a nominal scan length of 6 (9 eyes), 7 (107 eyes), or 8 (3 eyes) mm. For 31 eyes, no line scans were acquired; therefore, volume scans subtending nominal scan dimensions of 7×1 (30 eyes) or 7×2 mm (1 eye) were used for analysis instead. For the remaining two eyes, the line scan was not positioned at the fovea; therefore, a single B-scan was extracted from a volume scan (6×6 or 7×7 mm) and used for analysis. For all except these two eyes, multiple B-scans (n = 2–21) were registered and averaged to create a single .tif image for analysis, as described above.

OCT Analysis

To assess the OCT signal quality of the 236 images used for our symmetry analyses, the maximum tissue contrast index (mTCI) was computed for each image. The mTCI is a ratio between the signal intensity of the background and foreground pixels of an OCT image.[34] The background was defined as those pixels in the vitreous anterior to the inner limiting membrane (ILM) and the foreground was defined as those pixels in the retina and choroid posterior to the ILM. To implement the mTCI algorithm on our images, we obtained images of the noise profile of the Bioptigen OCT devices used for collecting the images in this study. Before computing the mTCI, the OCT images were cropped to position the center of the foveal pit at the center of the image in the axial dimension (i.e., there was an equal number of background and foreground pixels at the fovea).

The foveal ONL thickness was measured in the logarithmically-transformed image using a five-pixel wide longitudinal reflectivity profile (LRP) with custom software (OCT Reflectivity Analytics [ORA]).[29] The LRP measurements were made orthogonal to the retinal pigment epithelium layer at the center of the foveal depression, though six of the 236 images were tilted during acquisition and needed to be rotated before analysis since ORA only allows placement of vertically-oriented LRPs. In scans with complete foveal excavation, the boundaries of the ONL were selected from the peaks of the LRP corresponding to the ILM and the external limiting membrane (ELM; Fig. 1A). In scans with foveal hypoplasia, the posterior boundary of the outer

Table 2. ONL Statistics and Repeatability for ACHM and Control Subjects

	Control		ACHM	
	Right Eye	Left Eye	Right Eye	Left Eye
Mean ONL thickness, μm ± SD	112.9 ± 15.2	112.1 ± 13.9	79.7 ± 18.3	79.2 ± 18.7
Median ONL thickness, μm	112.7	114.5	77.6	75.8
Interquartile range, μm	20.0	21.2	20.4	23.7
ICC	0.976	0.982	0.925	0.935
95% CI	0.963–0.988	0.972–0.991	0.898–0.953	0.910–0.959
Repeatability (μm)[a]	6.62	5.27	14.2	13.6

[a] Defined as $2.77 \times S_w$.

plexiform layer (OPL) was used as the anterior boundary of the ONL instead of the ILM (Fig. 1B).[9,19,27] The distance between the two peaks, representing ONL thickness, was calculated and output by the software.[29] Three independent LRP estimates of foveal ONL thickness were obtained, with the single grader (RRM) masked to their prior measurements to assess repeatability. The mean of their three measurements was used for further analyses.

Statistical Analyses

Descriptive and comparative statistics were calculated using GraphPad Prism (v8, GraphPad Software, La Jolla, CA), with intraclass correlation coefficient (ICC) being estimated using R statistical software (R Statistical Software, Vienna, Austria). The repeatability was computed from the within-subject standard deviation (S_w) as described by Bland and Altman.[35] Data were tested for normality using the Shapiro-Wilk test to guide use of parametric or nonparametric statistical tests as appropriate.

Results

Subjects

As shown in Table 1, no statistical sex difference was observed between subjects with ACHM and controls ($P = 0.702$, Fisher's exact test). Although controls were older, on average, than subjects with ACHM (mean difference, 2.5 years), this was not a significant difference ($P = 0.064$, Mann-Whitney U test). Axial length for subjects with ACHM compared to controls also was not statistically different for either eye (right eye, $P = 0.166$; left eye, $P = 0.088$; Mann-Whitney U test). Furthermore, no significant interocular difference in axial length was observed for either the subjects with ACHM ($P = 0.084$, Wilcoxon matched-pairs test) or controls ($P = 0.827$, Wilcoxon matched-pairs test).

Foveal ONL Thickness Shows Excellent Repeatability

The high prevalence of hypoplasia and variable ellipsoid zone disruption can complicate the delineation of the ONL boundaries in patients with ACHM, possibly affecting the repeatability of such measures. Thus, it was important to establish the repeatability of our observer before progressing to studies of symmetry of our cohort. Our observer (RRM) showed excellent intraobserver repeatability, with ICC values for ACHM and control subjects shown in Table 2. Importantly, the 95% confidence intervals (CIs) for both eyes of the control subjects did not overlap with the CIs for the subjects with ACHM. This indicated that while both groups show excellent repeatability, measurements on the ACHM scans were slightly less repeatable than in controls. This also was seen in assessing the repeatability using the within subject standard deviation (S_w).[35] Repeatability was estimated as 2.7 times S_w, and the difference between any two measurements for the same subject is expected to be less than this value for 95% of pairs of observations.[35] As seen in Table 2, the repeatability was better in the control subjects (right eye = 6.62 μm, left eye = 5.27 μm) compared to the subjects with ACHM (right eye = 14.2 μm, left eye = 13.6 μm). These data may be useful for efforts to establish the degree of ONL change that should be considered significant when examining subjects with ACHM over time, as well as assessing the performance of different observers.

As mentioned above, the images used for analysis were comprised of 1 to 21 B scans; as such, the image quality was highly variable. This variability is representative of imaging a patient population with nystagmus. Therefore, we quantitatively characterized the image signal quality to assess whether our

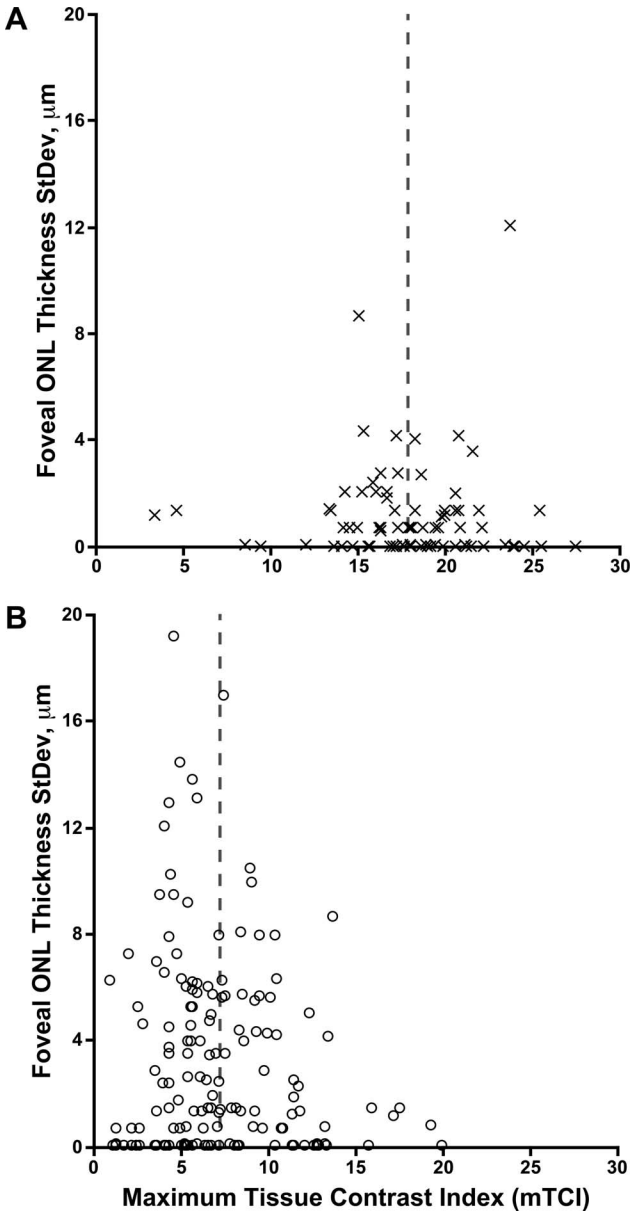

Figure 2. Relationship between image signal quality and repeatability of foveal ONL measurements. Plotted are mTCI values for each image against the standard deviation of the three repeated measurements of foveal ONL thickness for that same image for controls (A) and subjects with ACHM (B). Images from both eyes are included in each plot for a total of 84 and 152 images, respectively. The mean mTCI (*vertical dashed lines*) was higher in the images from control subjects compared to images from subjects with ACHM. However, no significant relationship between mTCI and observer repeatability was observed in either the images from controls (Spearman $r = -0.162$, 95% CI = −0.370–0.060, $P = 0.140$) or the subjects with ACHM (Spearman $r = -0.076$, 95% CI = −0.237–0.089, $P = 0.351$).

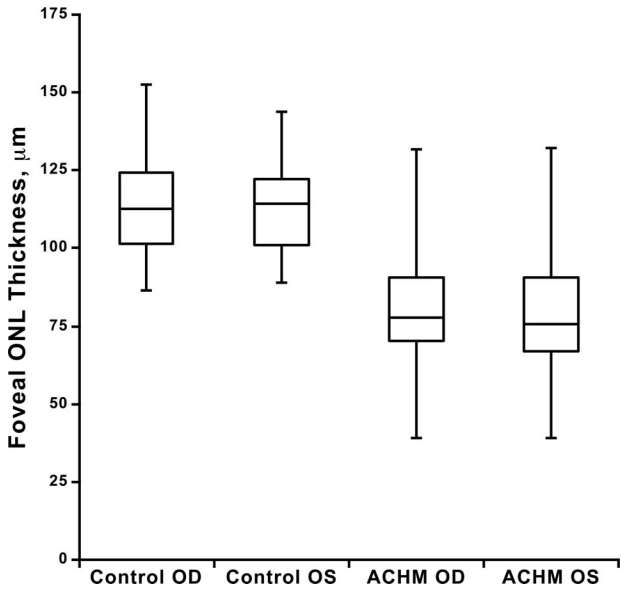

Figure 3. Foveal ONL thickness for both eyes of control and ACHM subjects. On average, subjects with ACHM have a thinner foveal ONL than controls ($P < 0.0001$, $t_{11} = 9.97$; right eye unpaired *t*-test), though there is substantial overlap between groups. Shown is the median for each group (*middle horizontal line*), while the 25th and 75th quartiles are represented by the *lower* and *upper rectangle* boundaries, respectively. *Error bars*: Extend to the minimum and maximum values within each group. Foveal ONL thickness did not differ between eyes in subjects with ACHM ($P = 0.636$, $t_{75} = 0.475$, paired *t*-test) or control subjects ($P = 0.434$, $t_{41} = 0.796$, paired *t*-test).

observer's repeatability was affected by the image signal quality. mTCI ranged from 3.31 to 27.5 for the controls and 1.02 to 20.0 for the subjects with ACHM. While the mTCI was lower on average for the ACHM images than those from controls ($P < 0.0001$, Mann Whitney *U* test), there was no significant relationship between mTCI for a given image and the intraobserver repeatability for that image (Fig. 2). Thus, at least in this group of subjects, the variable image quality did not appear to influence the observer performance.

Foveal ONL Thickness Shows High Interocular Symmetry

Consistent with previous reports,[19,26,27] subjects with ACHM had a thinner foveal ONL on average than control subjects ($P < 0.0001$, $t_{11} = 9.96$; right eye, unpaired *t*-test, Table 2, Fig. 3), though there was considerable overlap between the groups (Fig. 3). ONL thickness at the fovea did not differ between eyes in subjects with ACHM ($P = 0.636$, $t_{75} = 0.475$, paired *t*-test) or control subjects ($P = 0.434$, $t_{41} =$

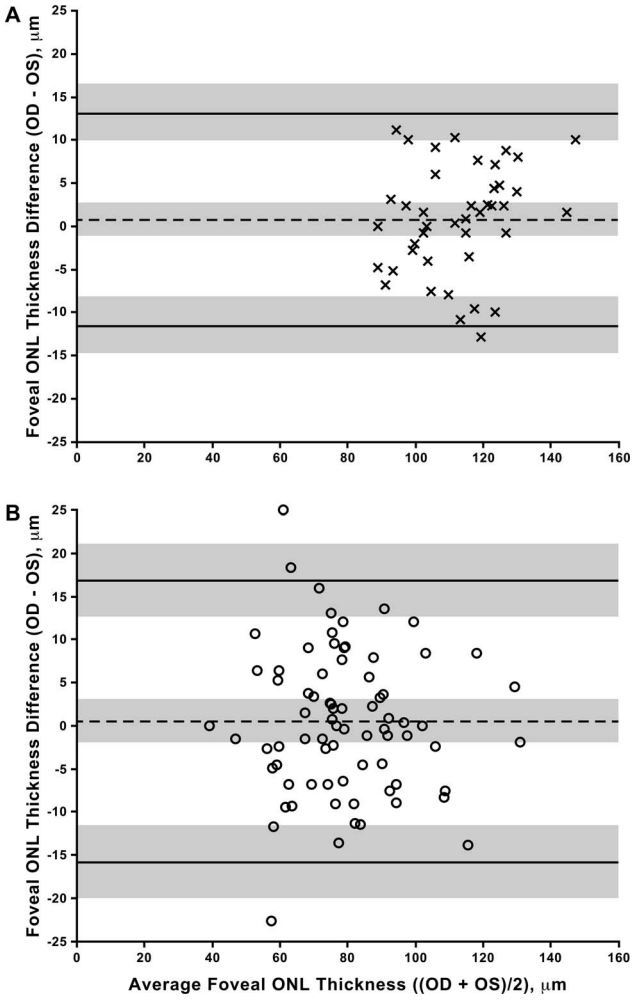

Figure 4. Interocular symmetry of foveal ONL thickness. Shown are Bland-Altman plots using data from controls (A) and subjects with ACHM (B). No significant bias was observed in either group. *Dashed line* represents average bias between the eyes, *solid lines* represent limits of agreement (LOA), gray shading represents CIs for the bias and LOAs.

0.796, paired *t*-test). In addition, the values from the right and left eyes were highly correlated for both the subjects with ACHM (Pearson $r = 0.899$, 95% CI = 0.845–0.935) and the control subjects (Pearson $r = 0.911$, 95% CI = 0.839–0.951). Taken together, these data indicate high interocular symmetry in both populations (Fig. 3). The Bland-Altman plots (Fig. 4) show that 95% of the interocular differences (right–left eyes) in our subjects fall between −11.5 and 13.1 μm for controls and −15.9 and 16.8 μm for the subjects with ACHM.

Though ONL symmetry was observed overall, there were subjects who had moderate differences in ONL thickness between eyes. Close inspection of the images from these subjects illustrates some potential confounds in extracting accurate ONL measurements from some images. Two examples are shown in Figure 5. The left eye of subject JC_0794 had a foveal ONL thickness that was 24.9 μm less than that measured in the right eye. While this may represent true asymmetry, the sharpness of the anterior ONL boundary is qualitatively worse in the left eye. Subject JC_10089 had the second greatest interocular difference (22.7 μm). Interestingly, the left eye of this subject had the ninth worse repeatability of the 152 ACHM images measured. The OPL is more evident in the right eye relative to the left eye, which may underlie the apparent asymmetry and poor repeatability of the left eye. Even though the overall trend supports symmetrical foveal ONL thickness across subjects, one must be aware of isolated cases of asymmetry.

Discussion

In this study, we identified that the ONL at the fovea was thinner in subjects with ACHM, consistent with previous studies.[19,21,26–28] The overlap between subjects with ACHM and controls highlights the significant variability that is present in ACHM. Additionally, the high repeatability of our ONL measurements suggests that the presence of foveal hypoplasia and variable image quality does not obviate robust assessment (at least by the observer used here) of foveal ONL thickness in this patient population, which often can be highly challenging to image with OCT and other modalities.

One limitation of our study is that the controls were slightly older than the ACHM population by an average of 2.6 years (though this was not statistically significant). Previous literature has conflicting reports of the effect of age on ONL measurements, with some reporting no significant changes,[36,37] some reporting thinning,[38] and some reporting thickening.[39,40] If ONL thickness decreases with age, then accounting for this within our study would only have further increased the significance of ONL thickness difference between the two groups. On the contrary, if ONL thickness increases with age, as suggested by Chui et al.,[39] this would amount to an increase in ONL thickness of less than 0.5 μm, given the 2.6-year age difference. As controls have a thicker ONL than subjects with ACHM by approximately 30 μm, the difference observed is most likely due to ACHM rather than any potential age changes. Another limitation was the retrospective nature of our study. In this regard, we essentially used whatever scans were available (which leaves a number of variables

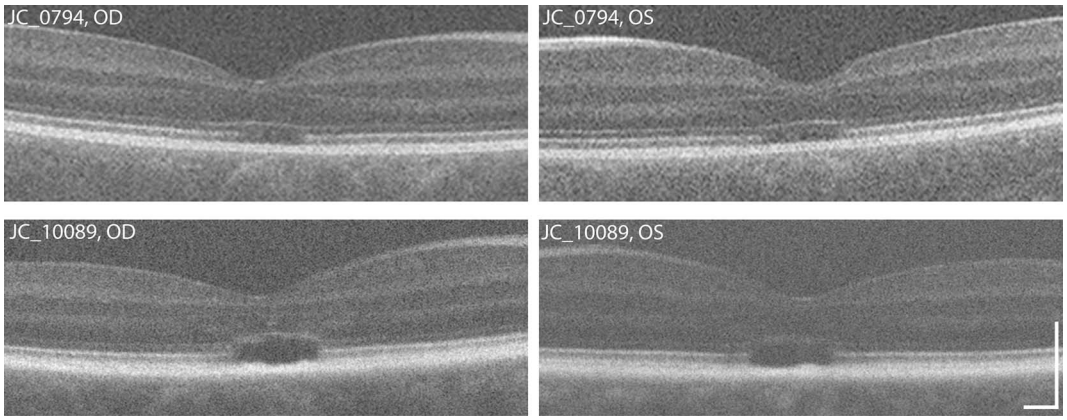

Figure 5. Examples of eyes with apparent interocular asymmetry. The right eye of subject JC_0794 (*top left*) had a foveal ONL thickness that was 24.9 μm greater than that measured in the left eye (*top right*). In this subject, the sharpness of the anterior ONL boundary is qualitatively worse in the left eye. ONL asymmetry also was observed in JC_10089, with the right eye (*bottom left*) being 22.7 μm less than that measured in the left eye (*bottom right*). In this subject, the low contrast of the OPL in the left eye likely played a role in this apparent asymmetry. *Scale bar*: 200 μm.

uncontrolled). However the reasons for some scans not being available in some subjects often is due to nystagmus, so excluding them may induce a selection bias in the overall analysis of the ONL.

Understanding the disease sequence for degenerating cone photoreceptors also is important. This has been observed previously using the progression of degenerating photoreceptors in retinitis pigmentosa. Reports exist of shortening outer segments and enlargement of inner segments occur before the final swelling of cone nuclei, directly preceding cone photoreceptor loss.[22–25] Moreover, Jacobson et al.[41] suggested there is a staging of cone degeneration in patients with Leber congenital amaurosis (LCA). They proposed that within a given disease, cone photoreceptors can be at varying stages of degeneration and often, regardless of intervention, some of them cannot be saved.[41] This hypothesis was supported by observations in an LCA clinical trial, of improved vision in treated patients, yet ONL thickness still was seen to decrease (suggestive of continued cone cell death progression).[41,42] Exactly how intact a cone must be to remain amenable to restoration of function via gene replacement therapy in ACHM is unknown. Comprehensive assessment of the integrity of remnant foveal cones may benefit from combining ONL thickness data with measurements of cone inner segment density (assessed directly using nonconfocal split-detector AOSLO) and outer segment integrity (as inferred from the relative cone reflectivity or waveguiding properties seen using confocal AOSLO).[18,19] Such data may help to paint a more complete picture of the therapeutic potential of a given retina, which could be of use in helping frame (on a personalized basis) patient and physician expectations regarding gene replacement therapy outcomes. However, a major obstacle remains: the fact that AOSLO imaging is only successful in approximately 55% of patients with ACHM obviates comparisons between these different measures of photoreceptor structure in many subjects.

In conclusion, subjects with ACHM have a thinner foveal ONL on average, though there is substantial variability between individuals. Our ONL thickness measurements derived from OCT showed minimal disparity in foveal ONL thickness between eyes, suggesting that the non-study eye can be used as a control in clinical trials.

Acknowledgments

The authors thank Brian Higgins, Alex Salmon, and Melissa Wilk for their contributions to this work.

Supported in part by the National Center for Advancing Translational Sciences of the National Institutes of Health (NIH; Bethesda, MD) under award number UL1TR001436, the National Eye Institute of the NIH under award numbers R01EY017607, P30EY001931, F32EY029148, and T32EY014537, and by the National Institute of General Medical Sciences of the NIH under award number T32GM080202. This investigation was conducted in part in a facility constructed with support from a Research Facilities Improvement Program,

grant number C06RR016511 from the National Center for Research Resources, NIH. The content is solely the responsibility of the authors and does not necessarily represent the official views of the National Institutes of Health. Additional support was provided by the Institute for Health Research, the Biomedical Research Centre at Moorfields Eye Hospital NHS Foundation Trust and UCL Institute of Ophthalmology, Fight for Sight, Moorfields Eye Hospital Special Trustees, Moorfields Eye Charity, Retinitis Pigmentosa Fighting Blindness, and the Foundation Fighting Blindness (USA).

Disclosure: **R.R. Mastey**, None; **M. Gaffney**, None; **K.M. Litts**, None; **C.S. Langlo**, None; **E.J. Patterson**, None; **M.R. Strampe**, None; **A. Kalitzeos**, None; **M. Michaelides**, MeiraGTx (C,F); **J. Carroll**, MeiraGTx (C,F), AGTC (F), Optovue (F)

References

1. Aboshiha J, Dubis AM, Carroll J, Hardcastle AJ, Michaelides M. The cone dysfunction syndromes. *Br J Ophthalmol*. 2016;100:115–121.
2. Kohl S, Baumann B, Rosenberg T, et al. Mutations in the cone photoreceptor G-protein α-subunit gene *GNAT2* in patients with achromatopsia. *Am J Hum Genet*. 2002;71:422–425.
3. Thiadens AA, Slingerland NW, Roosing S, et al. Genetic etiology and clinical consequences of complete and incomplete achromatopsia. *Ophthalmology*. 2009;116:1984–1989.
4. Kohl S, Coppieters F, Meire F, et al. A nonsense mutation in *PDE6H* causes autosomal-recessive incomplete achromatopsia. *Am J Hum Genet*. 2012;91:527–532.
5. Kohl S, Zobor D, Chiang W, et al. Mutations in the unfolded protein response regulator *ATF6* cause the cone dysfunction disorder achromatopsia. *Nat Genet*. 2015;47:757–765.
6. Kohl S, Varsanyi B, Antunes GA, et al. *CNGB3* mutations account for 50% of all cases with autosomal recessive achromatopsia. *Eur J Hum Genet*, 2005;13:302–308.
7. Thiadens AA, Somervuo V, van den Born LI, Roosing S, et al. Progressive loss of cones in achromatopsia: an imaging study using spectral-domain optical coherence tomography. *Invest Ophthalmol Vis Sci*. 2010;51:5952–5957.
8. Thomas MG, McLean RJ, Kohl S, Sheth V, Gottlob I. Early signs of longitudinal progressive cone photoreceptor degeneration in achromatopsia. *Br J Ophthalmol*. 2012;96:1232–1236.
9. Aboshiha J, Dubis AM, Cowing J, et al. A prospective longitudinal study of retinal structure and function in achromatopsia. *Invest Ophthalmol Vis Sci*. 2014;55:5733–5743.
10. Langlo CS, Erker LR, Parker M, et al. Repeatability and longitudinal assessment of foveal cone structure in *CNGB3*-associated achromatopsia. *Retina*. 2017;1956–1966.
11. Hirji N, Georgiou M, Kalitzeos A, et al. Longitudinal assessment of retinal structure in achromatopsia patients with long-term follow-up. *Invest Ophthalmol Vis Sci*. 2018;59:5735–5744.
12. Komáromy A, Alexander JJ, Rowlan JS, et al. Gene therapy rescues cone function in congenital achromatopsia. *Hum Mol Genet*. 2010;19:2581–2593.
13. Carvalho LS, Xu J, Pearson RA, et al. Long-term and age-dependent restoration of visual function in a mouse model of *CNGB3*-associated achromatopsia following gene therapy. *Hum Mol Genet*. 2011;20:3161–3175.
14. Banin E, Gootwine E, Obolensky A, et al. Gene augmentation therapy restores retinal function and visual behavior in a sheep model of *CNGA3* achromatopsia. *Mol Ther*. 2015;23:1423–1433.
15. Zobor D, Werner A, Stanzial F, et al. The clinical phenotype of *CNGA3*-related achromatopsia: pretreatment characterization in preparation of a gene replacement therapy trial. *Invest Ophthalmol Vis Sci*. 2017;58:821–832.
16. Michalakis S, Becirovic E, Biel M. Retinal cyclic nucleotide-gated channels: from pathophysiology to therapy. *Int J Mol Sci*. 2018;19:E749.
17. Genead MA, Fishman GA, Rha J, et al. Photoreceptor structure and function in patients with congenital achromatopsia. *Invest Ophthalmol Vis Sci*. 2011;52:7298–7308.
18. Dubis AM, Cooper RF, Aboshiha J, et al. Genotype-dependent variability in residual cone structure in achromatopsia: towards developing metrics for assessing cone health. *Invest Ophthalmol Vis Sci*. 2014;55:7303–7311.
19. Langlo CS, Patterson EJ, Higgins BP, et al. Residual foveal cone structure in *CNGB3*-associated achromatopsia. *Invest Ophthalmol Vis Sci*. 2016;57:3984–3995.
20. Scoles D, Sulai YN, Langlo CS, Fishman GA, Curcio CA, Carroll J, Dubra A. In vivo imaging of human cone photoreceptor inner segments. *Invest Ophthalmol Vis Sci*. 2014;55:4244–4251.

21. Georgiou M, Litts KM, Kalitzeos A, et al. Adaptive optics retinal imaging in *CNGA3*-associated achromatopsia: retinal characterization, interocular symmetry, and intrafamilial variability. *Invest Ophthalmol Vis Sci*. 2019;60:383–396.
22. Milam AH, Li ZY, Fariss RN. Histopathology of the human retina in retinitis pigmentosa. *Prog Retin Eye Res*. 1998;17:175–205.
23. Nork TM, Ver Hoeve JN, Poulsen GL, et al. Swelling and loss of photoreceptors in chronic human and experimental glaucomas. *Arch Ophthalmol*. 2000;118:235–245.
24. Murakami Y, Ikeda Y, Nakatake S, et al. Necrotic enlargement of cone photoreceptor cells and the release of high-mobility group box-1 in retinitis pigmentosa. *Cell Death Discharge*. 2015;15058.
25. Litts KM, Messinger JD, Freund KB, Zhang Y, Curcio CA. Inner segment remodeling and mitochondrial translocation in cone photoreceptors in age-related macular degeneration with outer retinal tubulation. *Invest Ophthalmol Vis Sci*. 2015;56:2243–2253.
26. Thomas MG, Kumar A, Kohl S, Proudlock FA, Gottlob I. High-resolution in vivo imaging in achromatopsia. *Ophthalmology*. 2011;118:882–887.
27. Sundaram V, Wilde C, Aboshiha J, et al. Retinal structure and function in achromatopsia: implications for gene therapy. *Ophthalmology*. 2014;121:234–245.
28. Yang P, Michaels KV, Courtney RJ, et al. Retinal morphology of patients with achromatopsia during early childhood: implications for gene therapy. *JAMA Ophthalmol*. 2014;132:823–831.
29. Wilk MA, Wilk BM, Langlo CS, Cooper RF, Carroll J. Evaluating outer segment length as a surrogate measure of peak foveal cone density. *Vision Res*. 2017;130:57–66.
30. Tanga L, Roberti G, Oddone F, et al. Evaluating the effect of pupil dilation on spectral-domain optical coherence tomography measurements and their quality score. *BMC Ophthalmol*. 2015;15:175.
31. Schneider CA, Rasband WS, Eliceiri KW. NIH image to ImageJ: 25 years of image analysis. *Nat Methods*. 2012;9:671–675.
32. Thévenaz P, Ruttimann UE, Unser M. A pyramid approach to subpixel registration based on intensity. *IEEE Trans Image Process*. 1998;7:27–41.
33. Tanna H, Dubis AM, Ayub N, et al. Retinal imaging using commercial broadband optical coherence tomography. *Br J Ophthalmol*. 2010;94:372–376.
34. Huang Y, Gangaputra S, Lee KE, et al. Signal quality assessment of retinal optical coherence tomography images. *Invest Ophthalmol Vis Sci*. 2012;53:2133–2141.
35. Bland JM, Altman DG. Measuring agreement in method comparison studies. *Stat Methods Med Res*. 1999;8:135–160.
36. Ooto S, Hangai M, Tomidokoro A, et al. Effects of age, sex, and axial length on the three-dimensional profile of normal macular layer structures. *Invest Ophthalmol Vis Sci*. 2011;52:8769–8779.
37. Won JY, Kim SE, Park YH. Effect of age and sex on retinal layer thickness and volume in normal eyes. *Medicine*. 2016;95:e5441.
38. Nieves-Moreno M, Martínez-de-la-Casa JM, Morales-Fernández L, Sánchez-Jean R, Sáenz-Francés F, García-Feijoó J. Impacts of age and sex on retinal layer thicknesses measured by spectral domain optical coherence tomography with Spectralis. *PLoS One*. 2018;13:e0194169.
39. Chui TY, Song H, Clark CA, Papay JA, Burns SA, Elsner AE. Cone photoreceptor packing density and the outer nuclear layer thickness in healthy subjects. *Invest Ophthalmol Vis Sci*. 2012;53:3545–3553.
40. Tong KK, Lujan BJ, Zhou Y, Lin MC. Directional optical coherence tomography reveals reliable outer nuclear layer measurements. *Optom Vis Sci*. 2016;93:714–719.
41. Jacobson SG, Cideciyan AV, Roman AJ, et al. Improvement and decline in vision with gene therapy in childhood blindness. *N Engl J Medical*. 2015;372:1920–1926.
42. Cideciyan AV, Jacobson SG, Beltran WA, et al. Human retinal gene therapy for Leber congenital amaurosis shows advancing retinal degeneration despite enduring visual improvement. *Proc Natl Acad Sci U S A*. 2013;110:E517–E525.
43. Staurenghi G, Sadda S, Chakravarthy U, Spaide RF, Panel IO. Proposed lexicon for anatomic landmarks in normal posterior segment spectral-domain optical coherence tomography: the IN•OCT consensus. *Ophthalmology*. 2014;121:1572–1578.